Electronic Supplementary Material (ESI) for Journal of Materials Chemistry B.

Supporting Information

Chitosan functionalized gold nanostar as theranostic platform for intracellular microRNA detection and photothermal therapy

*Xiaoxue Dong, Zongwei Zhu, Qian Sun, Hongqian Zhang, Chuanxu Yang**

Table S1. Sequences of DNA or RNA used

Name	Sequence 5'-3'
hpDNA	BHQ1-GCG CGT CAA CAT CAG TCT GAT AAG CTA CGC GC-FAM
fDNA	GCG CGT CAA CAT CAG TCT GAT AAG CTA CGC GC-FAM
dsDNA-Capturer	TCA ACA TCA GTC TGA TAA GCT A-BHQ1
dsDNA-Reporter	FAM-TAG CTT ATC AGA CTG A
miR21	UAG CUU AUC AGA CUG AUG UUG A
mis-miR21	UAG CUU AUG ACA GUG AUC UUG A
miR155	UUA AUG CUA AUU GUG AUA GGG GU
miR25	CAU UGC ACU UGU CUC GGU CUG A
miR93	CAA AGU GCU GUU CGU GCA GGU AG

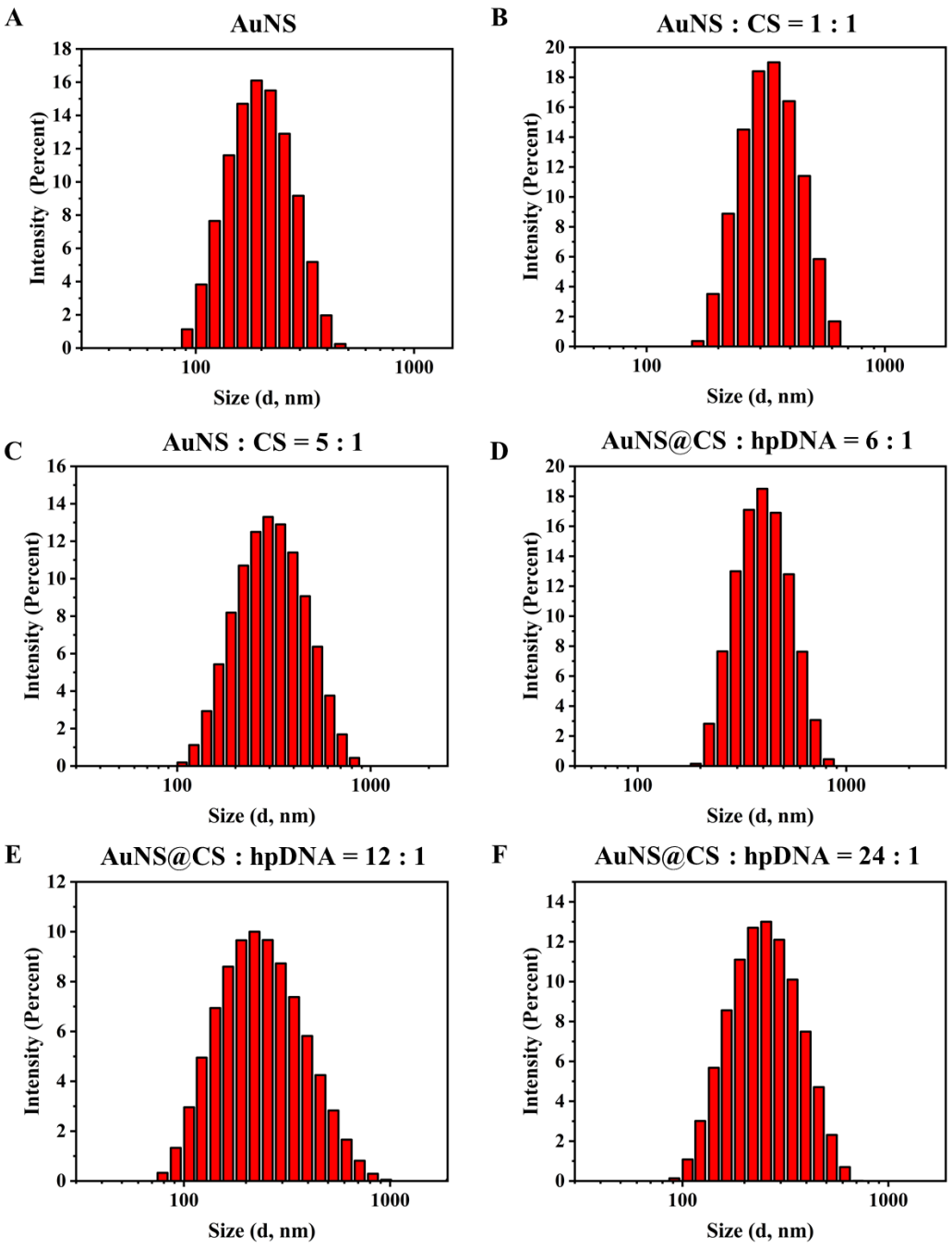

Figure S1. Representative histogram of size distribution measured by DLS.

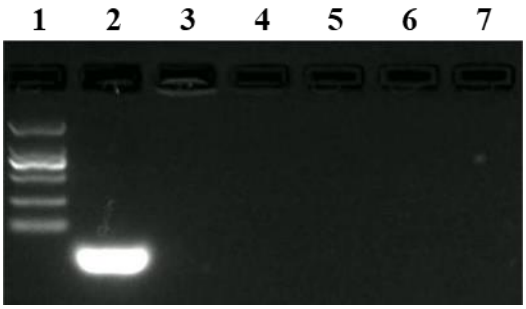

Figure S2. Gel electrophoresis analysis of hpDNA loading by AuNS@CS. Lane 1: DNA Maker; Lane 2: Free hpDNA; Lane 3: AuNS@CS : hpDNA = 1:1; Lane 4: AuNS@CS : hpDNA = 3:1; Lane 5: AuNS@CS : hpDNA = 6:1; Lane 6: AuNS@CS : hpDNA = 12:1; Lane 7: AuNS@CS : hpDNA = 24:1.

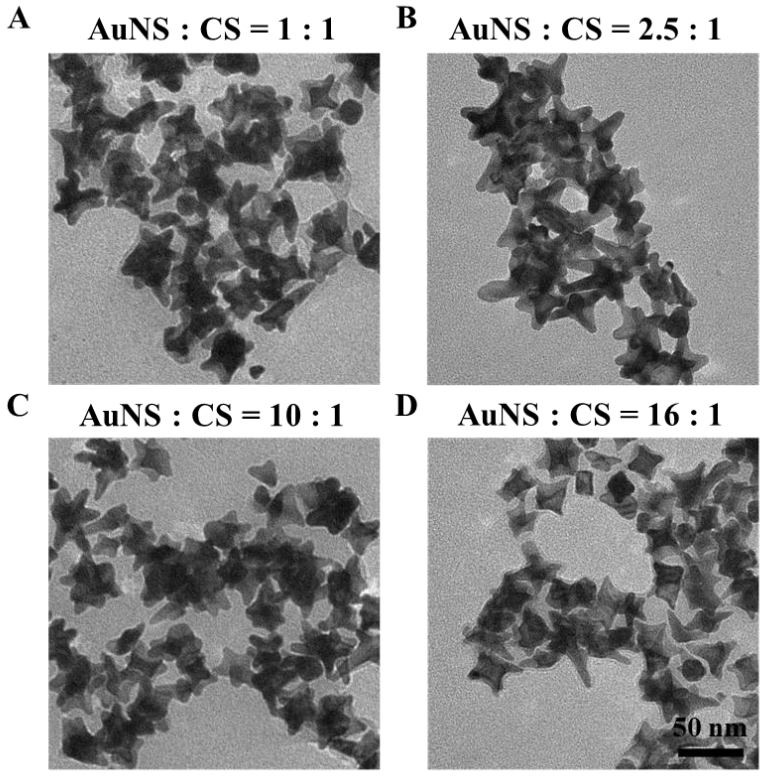

Figure S3. Transmission electron microscopy (TEM) images of AuNS@CS formulated at various weight ratios. Scale bars: 50 nm.

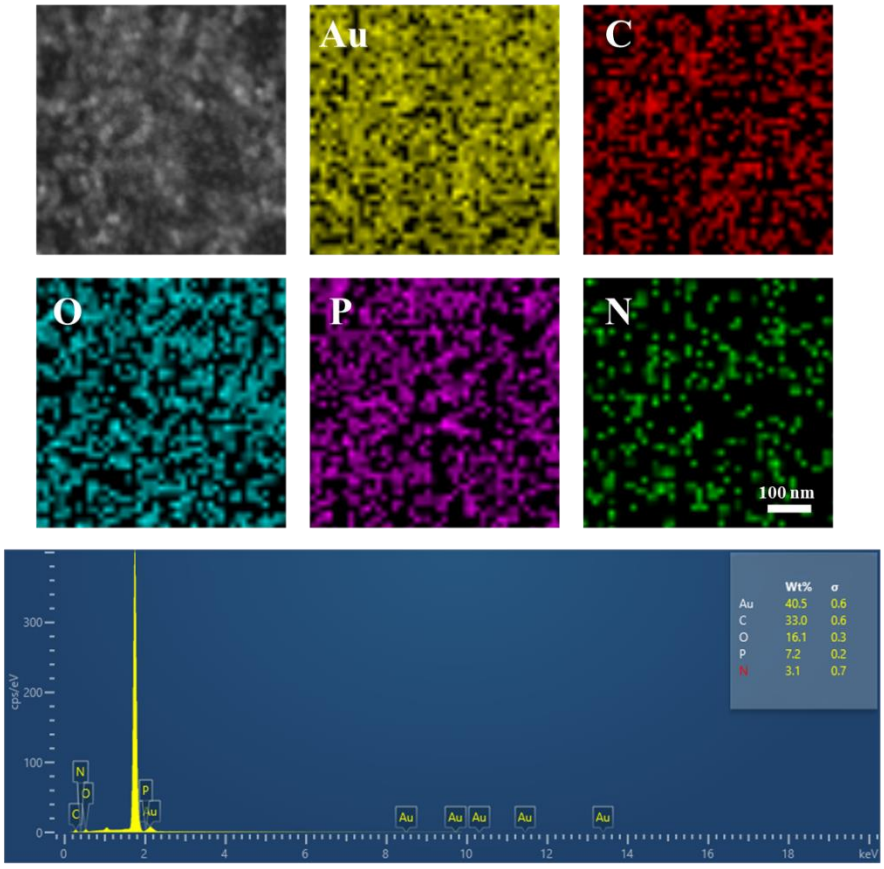

Figure S4. Representative SEM images, EDX elemental maps and EDX spectra of AuNS@CS-hpDNA.

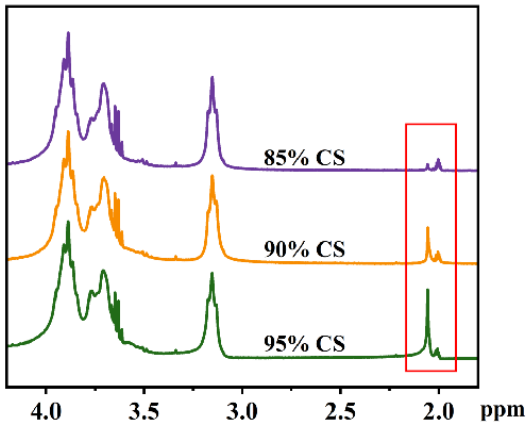

Figure S5. 1H NMR spectra of chitosan with different degrees of deacetylation.

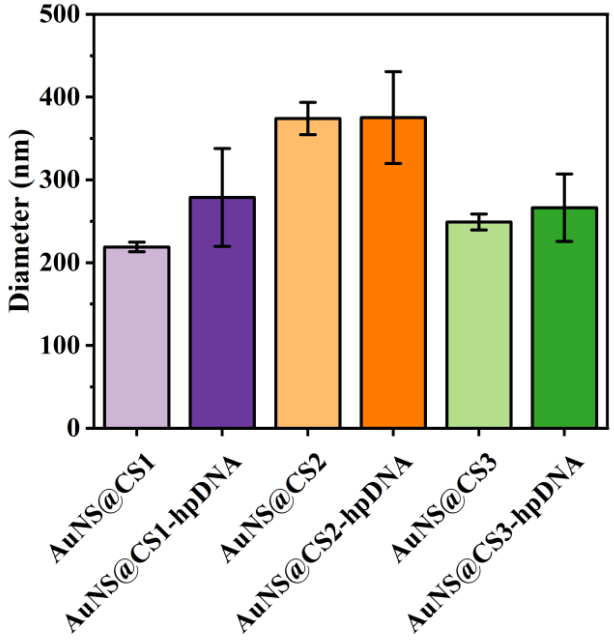

Figure S6. Diameter of the AuNS@CS and the AuNS@CS-hpDNA (AuNS@CS/hpDNA=12:1) formulated with different chitosan samples (CS1, CS2 and CS3) with degrees of deacetylation (85%, 90% and 95%). Error bars represent the means ± SD (n = 3).

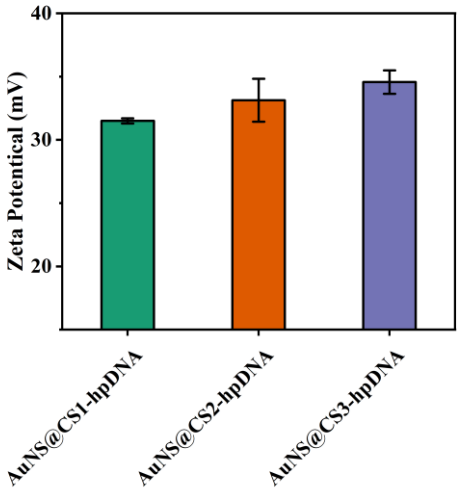

Figure S7. Zeta potential of AuNS@CS-hpDNA with different degrees of deacetylation (CS1, 85%; CS2, 90%; CS3, 95%).

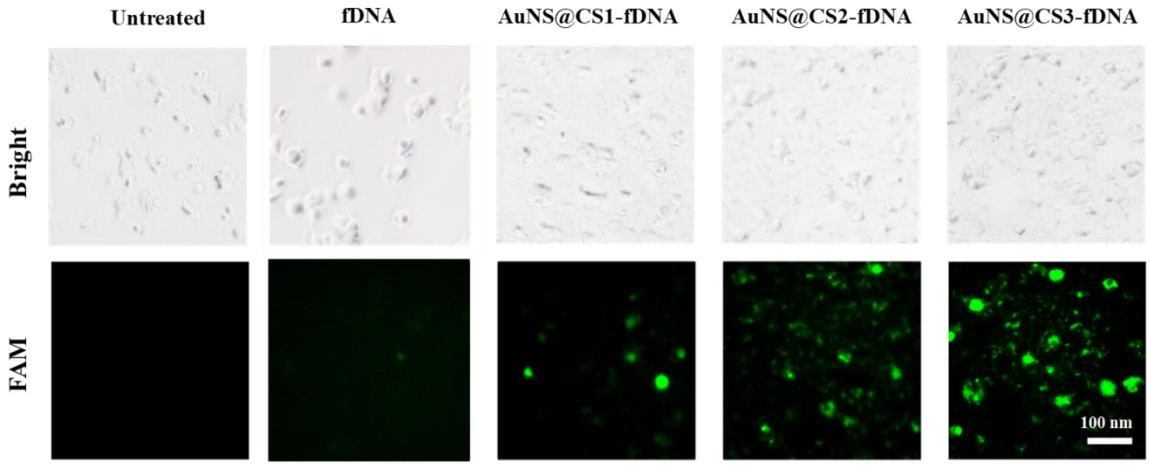

Figure S8. Cellular uptake of AuNS@CS-fDNA. Fluorescence microscope images displayed MCF-7 cells transfected with naked fluorescent hpDNA (fDNA) or AuNS@CS-fDNA formulated with different chitosan samples (CS1, CS2 and CS3) with deacetylation degrees (85%, 90% and 95%).

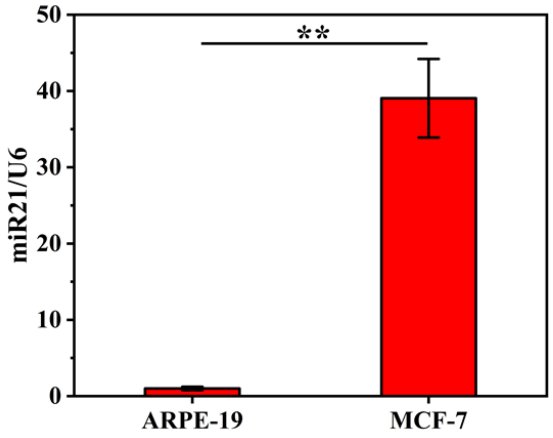

Figure S9. Expression level of miR21 expression levels in MCF-7 cells and ARPE-19 cells. U6 snRNA was utilized as control. Error bars represent the means ± SD (n = 5). ** $p < 0.01$.

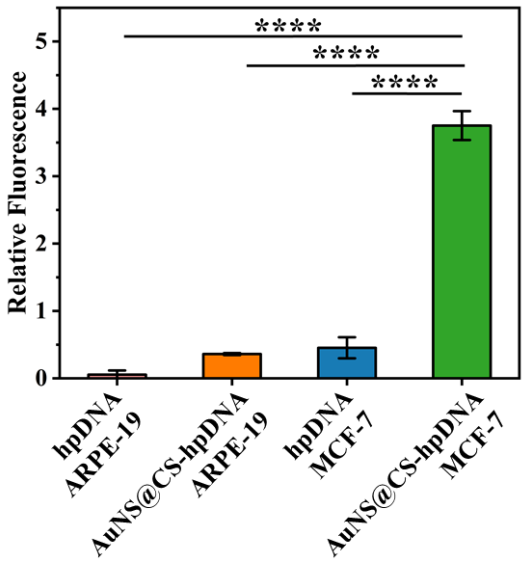

Figure S10. Quantification the intracellular fluorescence of hpDNA from fluorescence imaging. Fluorescence signals from ARPE-19 or MCF-7 cells with indicated treatment were quantified from the mean fluorescent intensity of sufficient number of cells. Statistical difference, **** $p < 0.0001$.

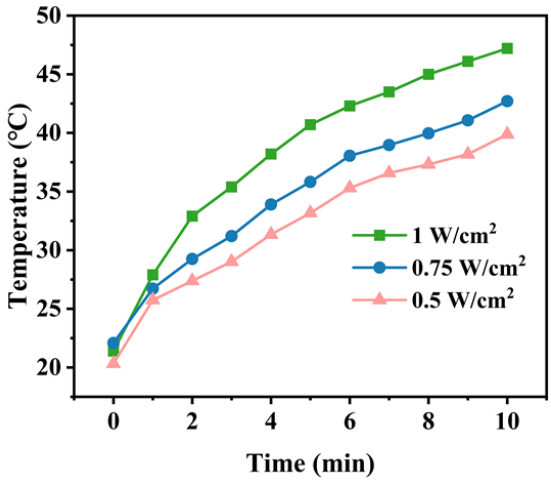

Figure S11. Temperature change curves of AuNS@CS during NIR laser irradiation with various laser power density.

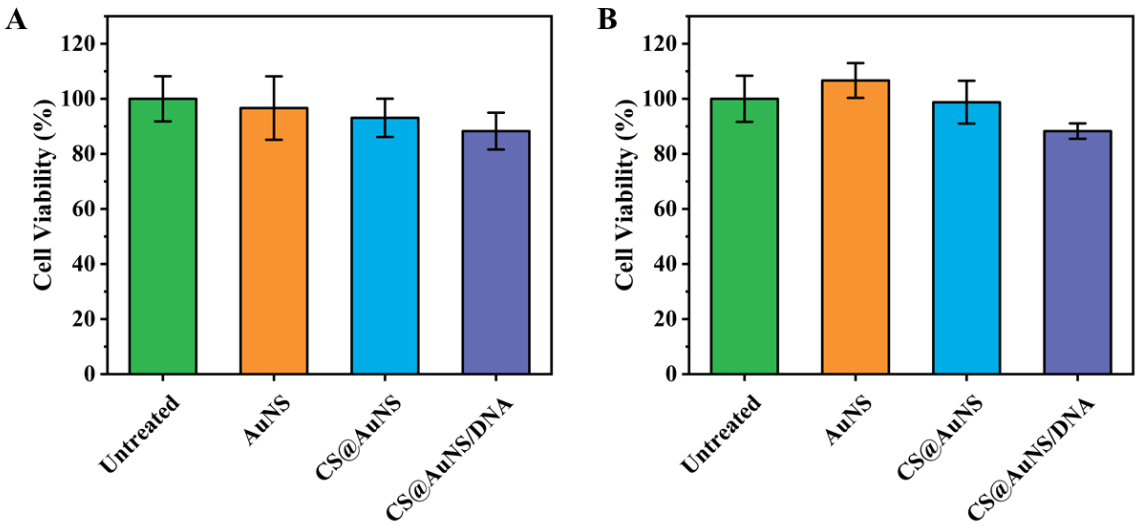

Figure S12. Cytotoxicity of AuNS, AuNS@CS and AuNS@CS-hpDNA on (A) MCF-7 and (B) ARPE-19 cells. Error bars represent the means ± SD (n = 5)